Eur. Phys. J. C 46, 421–428 (2006)
Digital Object Identifier (DOI) 10.1140/epjc/s2006-02499-4

THE EUROPEAN PHYSICAL JOURNAL C

A description of the ratio between electric and magnetic proton form factors by using space-like, time-like data and dispersion relations

R. Baldini[1,2], C. Bini[3], P. Gauzzi[3], M. Mirazita[2], M. Negrini[4], S. Pacetti[2,a]

[1] Centro Studi e Ricerche Enrico Fermi, Roma, Italy
[2] Laboratori Nazionali di Frascati dell'INFN, Frascati, Italy
[3] Università "La Sapienza" e Sezione INFN, Roma, Italy
[4] Università di Ferrara e Sezione INFN, Ferrara, Italy

Received: 8 July 2005 /
Published online: 31 March 2006 –

Abstract. We use the available information on the ratio between the electric and magnetic proton form factors coming from recently published space-like data and from the few available time-like data. We apply a dispersive procedure on these data to evaluate the behavior of this ratio, as a complex function, for all values of q^2.

1 Introduction

The electromagnetic form factors (ff's) are essential pieces of our knowledge of the internal structure of the nucleon, and this fact justifies the efforts devoted to their determination. They are complex functions of the squared momentum transfer in the photon–nucleon vertex, defined both for space-like ($q^2 < 0$) and time-like ($q^2 > 0$) momenta. The interest in the study of the nucleon ff's has been recently renewed [1, 2] by the unexpected Jlab results on the ratio

$$R(q^2) = \mu_p \frac{G_{\rm E}^p(q^2)}{G_{\rm M}^p(q^2)}\,, \tag{1}$$

where μ_p is the proton's magnetic moment and $G_{\rm E}^p$ and $G_{\rm M}^p$ are the electric and magnetic proton ff's. A decrease of $R(q^2)$ as space-like $\left|q^2\right|$ increases [3] has been found, in contrast with the flat behavior $R(q^2) \approx 1$ [4] obtained up to $q^2 \approx -7\,{\rm GeV}^2$ by using the traditional Rosenbluth method [5]. It has to be mentioned that the Iachello–Jackson–Lande (IJL) nucleon ff's model [6, 7], somehow related to soliton models of the nucleon [8], predicted the decrease of $R(q^2)$ more than thirty years ago. Recently this model [7] and other QCD based models [1, 9, 10] have been extrapolated to time-like positive q^2. While they agree within the experimental errors in the space-like region, they disagree in some respect for time-like q^2. In all these models the space-like q^2 variation is related to a cancellation between the Dirac, $F_1^p(q^2)$, and the Pauli, $F_2^p(q^2)$, ff's. Then, since we have

$$\begin{aligned} G_{\rm E}^p(q^2) &= F_1^p(q) + \tau F_2^p(q^2), \\ G_{\rm M}^p(q^2) &= F_1^p(q) + F_2^p(q^2), \end{aligned} \qquad \tau = \frac{q^2}{4M_p^2}, \tag{2}$$

such a cancellation should become an enhancement once q^2 (i.e. τ) changes sign from negative to positive time-like values. As a consequence the angular distribution of the outgoing nucleon in $e^+e^- \to N\overline{N}$ processes should have a large $\sin^2(\theta)$ term proportional to $\left|R(q^2)\right|^2$. At the same time, a large transverse polarization of the outgoing nucleon [11] is predicted [1], but the sign and the q^2-dependence strongly depend on the models.

In principle, time-like ff's could be evaluated from the space-like ones by means of dispersion relations (DR's), if they are smooth enough and if space-like data were known with very high accuracy or if in the time-like region there are some data or suitable constraints [12–14]. In fact, analytic functions are supposed to describe at the same time space-like and time-like electric and magnetic ff's. These functions are defined in the whole q^2 complex plane; in the physical sheet they do not have isolated singularities, such as poles, but a cut on the real axis starting at $s_\pi = (2m_\pi)^2$. The Cauchy theorem allows one to relate the space-like real values of a ff to an integral, over the time-like cut, of its imaginary part, providing a DR among them. In the unphysical region, $0 < q^2 < 4M_p^2$, not directly accessible experimentally, each ff should have large bumps corresponding to the unphysical excitations of ϱ, ω, ϱ', ω' and all vector mesons whose masses are lower than $2M_p$ [15]. In terms of ff's, these resonances are described by poles lying in the unphysical sheet of the q^2 complex plane. In the

[a] e-mail: simone.pacetti@lnf.infn.it

ratio $R(q^2)$ the effects of these poles should be somewhat smoothed out, being the same in both, $G_{\rm E}^p$ and $G_{\rm M}^p$. Hence $R(q^2)$ smoothness should be a plausible ansatz.

There are constraints to $R(q^2)$ for time-like q^2, namely:

- a continuous transition is expected from space-like to time-like q^2;
- according to the Phragmèn–Lindelöff theorem the space-like and time-like values of a ff must be asymptotically real and equal in modulus[16–18];
- at $q^2 = s_p \equiv (2M_p)^2$, the physical threshold of $e^+e^- \to p\bar{p}$, assuming $F_1^p(q^2)$ and $F_2^p(q^2)$ analytic functions of q^2, it is $R(s_p) = \mu_p$; since in this q^2 region $R(q^2)$ is a complex function, this is a constraint on both real and imaginary part.

All the published data in the time-like region assumed $\left|R(q^2)\right| = \mu_p$ not only at threshold [19–25], but in the whole explored interval [26–28], essentially for lack of accurate data concerning the angular distributions and of any measurement of the outgoing nucleon polarization or any use of polarized beams.

In this paper, the ratio $R(q^2)$ has been obtained in a model independent way, assuming it has a smooth behavior, taking into account the theoretical constraints and solving the DR by a minimization algorithm. The input of this algorithm is given by the JLab and MIT-Bates polarization data [3, 29] in the space-like region and by the result of a reanalysis of FENICE [19, 20], DM2 [21, 22] and E835 [30] data in the time-like region. A preliminary version [31] of this paper has been previously presented.

A very similar approach, even if with a different dispersive integral, has already been successfully tested on the pion ff [13]. In short, the pion ff has been assumed to be known in the space-like region and in the time-like region, above s_p only. Hence the DR has been reversed evaluating the time-like pion ff below s_p by means of a standard regularization procedure used to solve first kind integral equations, that requires one free parameter only [32]. A very good agreement has been obtained in this way, varying this parameter within one order of magnitude. This procedure has also been applied quite successfully to get the magnetic nucleon ff's in the unphysical region [13].

2 Space-like and time-like experimental data

The high intensity–high polarization electron beams available at JLab and MIT-Bates [3, 29] allowed the extraction of the ratio between electric and magnetic proton ff's measuring the electron-to-proton polarization transfer. These measurements showed an almost linear decrease of $R(Q^2)$ from unity at low $Q^2 \equiv -q^2$ up to ≈ 0.3 at the highest Q^2, as shown in Fig. 1, in strong disagreement with previous Rosenbluth measurements (see [4] and [33] for a compilation of all the space-like data), that indicated approximate ff scaling, i.e. $R(Q^2) \approx 1$, though with large uncertainties in $G_{\rm E}^p$ at the highest Q^2 values. In the Rosenbluth measurements, the ff's are basically extracted fitting the linear ϵ-dependence of the cross section at fixed Q^2 (where ϵ is the virtual photon polarization), but the presence of the factor $1/\tau$ [see (3)] in front of $G_{\rm E}^p(Q^2)$ makes difficult its extraction when Q^2 becomes large. Then, a possible experimental inconsistency could affect the Rosenbluth result, however a recent reanalysis [33] showed that the individual Rosenbluth measurements are consistent to each other within a small normalization uncertainty between the different experiments. In addition, the new Rosenbluth measurements performed at JLab [34] confirmed the scaling behavior of the old data for Q^2 from 2.6 to 4.1 GeV^2, making it clear that the source of the discrepancy is not simply experimental.

Recent theoretical works [35] have suggested that terms, related to two-photon exchange corrections to the lowest order QED diagram, may result in an incorrect determination of the ff's from the measured cross section,

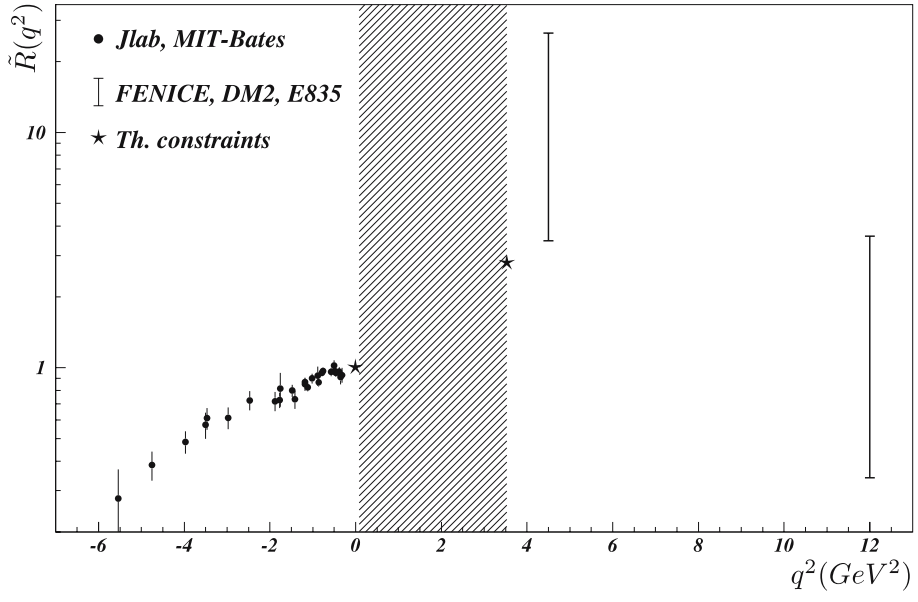

Fig. 1. The *full circles* represent the data from Jlab and MIT-Bates [3, 29], while the two time-like intervals are from FENICE [19, 20], DM2 [21, 22] and E835 [30]. The *stars* are the theoretical constraints and the lined area is the unphysical region. The label $\tilde{R}(q^2)$ of the ordinate axis is defined as $\tilde{R}(q^2) = R(q^2)$ for $q^2 \le s_\pi$ and $\tilde{R}(q^2) = \left|R(q^2)\right|$ for $q^2 > s_\pi$

while polarization measurements should be less sensitive to such corrections. As shown in [36], the Rosenbluth data with the inclusion of two-photon exchange contribution agree well with polarization data for Q^2 between 2 and 3 GeV^2, while there is at least partial reconciliation for higher Q^2. Once reliable calculations of these corrections will be available, then polarization and cross section data can be consistently combined to extract the ff's without ambiguity.

In our following analysis, we will make use of the ratio $R(Q^2)$ as obtained from polarization measurements, since, as discussed, these data are less sensitive to higher order corrections and to systematic uncertainties.

The proton ff's in the time-like region ($q^2 \equiv s > 0$) can be extracted from the cross section of the process $e^+e^- \to p\overline{p}$ or $p\overline{p} \to e^+e^-$. The measurements available from both kinds of experiments are shown in Fig. 2 as a function of the center of mass energy s. Most of the data are concentrated in the low s region close to the proton–antiproton threshold [19–25], but a sizeable amount of data from proton–antiproton annihilation experiments is also available for center of mass energies s between 8 and 14 GeV^2 [26–28]. The total cross section at a given s is related to the ff's $|G_{\rm E}^p(s)|$ and $|G_{\rm M}^p(s)|$ through the relation

$$\sigma(s) = \frac{4\pi\alpha^2\varrho(s)}{3s}\left(|G_{\rm M}^p(s)|^2 + \frac{2M_p^2}{s}|G_{\rm E}^p(s)|^2\right), \qquad (3)$$

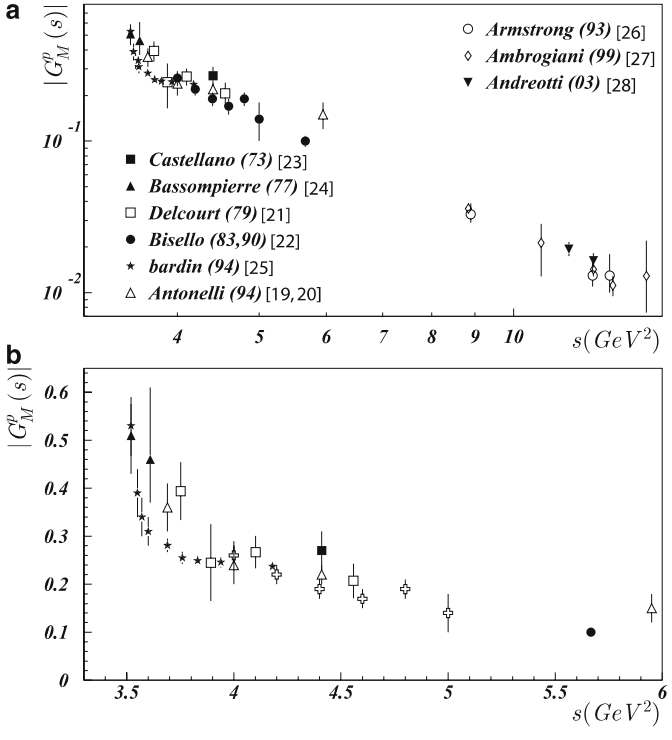

Fig. 2. Proton magnetic ff in the time-like region extracted from the $e^+e^- \to p\overline{p}$ and $p\overline{p} \to e^+e^-$ cross sections assuming $|G_{\rm E}^p(s)| = |G_{\rm M}^p(s)|$. **a** All data in logarithmic scale. **b** Data close to $s_p = (2M_p)^2$ in linear scale

where the factor $\varrho(s)$ is equal to $C\beta = Cv/c$ (v is the proton velocity in the center of mass system) in the case of $e^+e^- \to p\overline{p}$ and to β/C in the case of $p\overline{p} \to e^+e^-$ and C is a Coulomb correction factor to take into account QED bound states, relevant only very near threshold. In order to extract the ff's from the measured cross sections, each experiment has to make an hypothesis on the modulus of the ratio $R(s)$. All the results published are obtained in the hypothesis that this ratio, in modulus, is equal to μ_p ($|G_{\rm E}^p(s)| = |G_{\rm M}^p(s)|$).

The possibility to disentangle $|G_{\rm E}^p(s)|$ and $|G_{\rm M}^p(s)|$ relies on the measurement of the angular distributions. Calling θ the polar angle of the emerging proton (or antiproton) in the center of mass system in $e^+e^- \to p\overline{p}$ experiments, or the polar angle of the electron (or positron) in $p\overline{p} \to e^+e^-$ experiments, the differential cross section is

$$\frac{{\rm d}\sigma}{{\rm d}\Omega} = \frac{\alpha^2\varrho(s)}{4s}\left[|G_{\rm M}^p(s)|^2(1+\cos^2(\theta)) + \frac{1}{\tau}|G_{\rm E}^p(s)|^2\sin^2(\theta)\right], \qquad (4)$$

where $\tau = s/4M_p^2$. This formula shows that the two ff's give rise to two terms: one, related to the magnetic ff, has a $[1+\cos^2(\theta)]$-dependence, the other one, related to the electric ff has a $\sin^2(\theta)$-dependence. In principle a measurement of the angular distribution is able to give the relative weights of the two terms and hence the ratio $|R(s)|$. A fit of the $\cos(\theta)$ distributions has been applied to two sets of data corresponding to two different values of s.

1. The data from the FENICE [20] and DM2 [22] experiments both detecting the process $e^+e^- \to p\overline{p}$ at an average center of mass energy $s = 4.51$ GeV^2 have been simultaneously fitted. The two measured differential cross sections are in good agreement as shown in Fig. 3a.
2. Two sets of data from the E835 experiment [27, 28] detecting the process $p\overline{p} \to e^+e^-$ both at $s \sim 12$ GeV^2 have also been fitted simultaneously. The angular distributions of the two data sets are shown in Fig. 3b normalized to the average number of events per bin.

All the considered experiments are characterized by limited statistics due to the small value of the cross section (from ~ 1 nb at $s^{\rm exp} = 4.5$ GeV^2 down to ~ 1 pb at $s^{\rm exp} = 12$ GeV^2). In both cases the parameter $|R|^{\rm exp}$ is extracted from a fit to the c.m. angular distribution with

$$f(\cos(\theta)) = \tau\mu_p^2 A^2(1+\cos^2(\theta)) + B^2(1-\cos^2(\theta)), \qquad (5)$$

and the ratio between the two coefficients B and A is just $|R|^{\rm exp}$. In order to evaluate confidence intervals for $|R|^{\rm exp}$, properly taking into account the unavoidable correlations, the same fits have been applied on samples of distributions randomly extracted from the experimental ones. This procedure allows one to get directly the distributions of $|R|^{\rm exp}$. These are not Gaussian, being in both cases strongly asymmetric. Confidence intervals of 68% ($R^{\rm inf} < |R|^{\rm exp} < R^{\rm sup}$) are built in such a way that the probability $P(|R| > R^{\rm sup}) = P(|R| < R^{\rm inf}) = 16\%$.

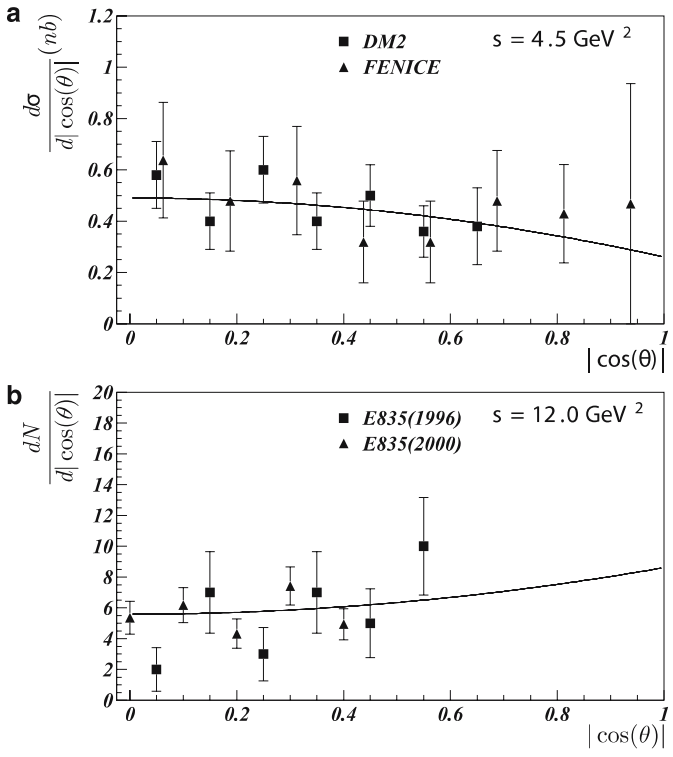

Fig. 3. **a** Differential cross section as a function of $|\cos(\theta)|$ from FENICE [19, 20] (*triangles*) and DM2 [21, 22] (*squares*) data at $s^{\rm exp} = 4.5\,{\rm GeV}^2$, with fit superimposed. **b** Angular distributions for E835 1996 data (*squares*) and 2000 data [30] (*triangles*) at $s^{\rm exp} = 12.0\,{\rm GeV}^2$, with fit superimposed: the two distributions are normalized to the same number of events per unit of $|\cos(\theta)|$

The resulting intervals are

$$\begin{aligned} 3.46 < |R|^{\rm exp} < 26.5 \quad & (s^{\rm exp} = 4.5\,{\rm GeV}^2), \\ 0.34 < |R|^{\rm exp} < 3.63 \quad & (s^{\rm exp} = 12.0\,{\rm GeV}^2). \end{aligned} \tag{6}$$

These numbers could be modified by taking into account the contribution of two-photon exchange diagrams, that should lead to an asymmetry in the angular distribution of the proton with respect to the antiproton. An effect of the order of few percent could be estimated, also taking into account that the $\gamma\gamma \to p\bar{p}$ cross section is of the same order of magnitude as for $e^+e^- \to p\bar{p}$ [37]. However, given the experimental uncertainties in the determination of the two intervals of (6), we do not expect that our final result will be affected by these higher order corrections.

3 The dispersive approach

In order to connect the data on $|R(s)|$ in the time-like region to those on $R(t)$ in the space-like region ($t = q^2 < 0$), we use a very powerful mathematical tool, i.e. the DR's for the imaginary part. They have the form [16]

$$G(t) = \frac{1}{\pi}\int_{s_\pi}^{\infty} \frac{{\rm Im}G(s)}{s-t}{\rm d}s\,. \tag{7}$$

Equation (7) establishes an integral relation between the values of the ff in the space-like region, where this function is real since it describes the scattering process, and its imaginary part in the time-like region, where the process described is the annihilation and therefore the ff is complex. If we assume that the magnetic proton ff $G_{\rm M}^p(q^2)$ has no zeros, as it is demonstrated in [13], it follows that, unless there is asymptotic behavior, the ratio $R(q^2)$ has the same analytic properties as of each ff. This means that we may apply the DR of (7) directly to $R(q^2)$. But, since pQCD [17] constrains the ff's $G_{\rm E}^p(q^2)$ and $G_{\rm M}^p(q^2)$ to be asymptotically vanishing with the same power law $(1/q^2)^2$, as q^2 diverges, the ratio, unless there are logarithmic corrections, should have a constant asymptotic time-like limit and therefore the integral of (7), with $R(s)$ instead of $G(s)$, could be divergent. In order to account for this possibility we perform the analytic continuation of $R(q^2)$ by means of the DR for the imaginary part, subtracted at $t = 0$ [16]:

$$R(t) = R(0) + \frac{t}{\pi}\int_{s_\pi}^{\infty} \frac{{\rm Im}[R(s)]}{s(s-t)}{\rm d}s\,, \tag{8}$$

which relates the space-like value of $R(t)$ to its time-like imaginary part, and

$${\rm Re}[R(s)] = R(0) + \frac{s}{\pi}\mathcal{P}\!\!\int_{s_\pi}^{\infty} \frac{{\rm Im}[R(s')]}{s'(s'-s)}{\rm d}s'\,, \tag{9}$$

which, instead, connects the real and the imaginary parts of $R(s)$ over the cut, i.e., for $s \geq s_\pi$ ($\mathcal{P}$ denotes the principal value). The price of the subtraction at $t = 0$ is the knowledge of the value of $R(t)$ at the same point, but, thanks to the normalization [see (1)], in the expressions (8) and (9) we can put $R(0) = 1$.

Contrary to the existing models [1, 6, 7, 9, 10], which are constructed starting from the space-like data and only subsequently extended to other energies, we start from the imaginary part of the ratio $R(s)$, which is defined only in the portion of the time-like region over the cut, and, by means of a rigorous analytic continuation procedure, we reconstruct the function $R(q^2)$ in the whole q^2 complex plane.

To parametrize the imaginary part we use a quite general and model independent form, that is, two series of orthogonal Chebyshev polynomials [16]:

$${\rm Im}R(s) = \begin{cases} \sum_j C_j T_j(x) x = \frac{2s - s_p - s_\pi}{s_p - s_\pi}, & s_\pi \leq s \leq s_p, \\ \sum_j D_j T_j(y) y = \frac{2s_p}{s} - 1, & s > s_p, \end{cases} \tag{10}$$

with $s \geq s_\pi$, the two vectors $\mathbf{C} = (C_1, C_2, \ldots, C_M)$ and $\mathbf{D} = (D_1, D_2, \ldots, D_N)$ represent the coefficients and $T_j(x)$ is the j-th Chebyshev polynomial. The two series in (10) cover two naturally separated intervals:

- the unphysical region $[s_\pi, s_p]$ with the vector meson resonances, where the ff's cannot be measured;
- the experimentally accessible region (s_p, ∞), where the asymptotic regime is attained.

Once ${\rm Im}[R(s)]$ is defined, $R(q^2)$ can be evaluated in the full q^2 range via (8) and (9). In order to find the $\mathbf{C}$ and

D vectors we minimize a χ^2 function that includes space-like and time-like data together with the constraints discussed above. The resulting function has the correct analytic structure.

It is interesting to see how the theoretical constraints, which can be imposed directly on the imaginary part of $R(q^2)$, are essentially three nodes located at three critical points, the theoretical thresholds s_π, the physical threshold s_p and the point at infinity, which are just the extremes of the domains of the series.

In order to choose the values for N and M, the degrees of the two series, we have studied the $\chi^2(N,M)$ as a function of (N,M) in the parameter space $([3,8]\times[4,9])$. In this space the χ^2 has an absolute minimum for $(N,M)=(5,6)$. Then, in the following, we will consider only this case, also because it lies in a region of stability, i.e., if we vary N and M by ±1 we obtain a result, which is within the errors in agreement with that obtained for $(N,M)=(5,6)$. The error, shown as a lined band in the pictures, has been achieved using a Monte Carlo technique, generating new sets of data, by means of Gaussian fluctuations from the original.

More details on the minimization procedure are reported in [38].

Concerning the dispersive procedure, it is interesting to mention that, in addition to the one adopted here, there are other forms of DR's which connect space-like and time-like data. For instance, the DR for the logarithm may relate directly data on the modulus of a ff in the time-like region to those for its real value in the space-like region [12, 13, 16]. This kind of logarithmic dispersive approach would not be suitable in this case, not only because the time-like modulus has not so many constraints as the imaginary part does, but also because it is not able to forecast, in a model independent way, the presence of a zero, that, instead, should be one of the aims of this analysis.

In the pictures of Fig. 4 is shown our result for the ratio $R(q^2)$, also in comparison with some existing models [1, 6, 7, 9, 10].

In particular the IJL model [6, 7] represents a surprisingly accurate and early prediction of the space-like decreasing behavior of the ratio $R(q^2)$. However in these models the transition from space-like ff's to time-like ff's is essentially achieved by changing sign of q^2 and adding a phase. This recipe fulfills the analyticity requirement asymptotically. Conversely, in our procedure the analyticity in the whole q^2-plane is the first feature. In fact we parameterize directly the imaginary part of the ratio $R(q^2)$ and then we extend the definition in the whole q^2 complex plane by means of a rigorous analytic continuation technique based on the dispersion relations. The free parameters of this procedure are then fixed by using both theoretical and experimental constraints. In light of this, the function that comes out fulfills all the theoretical and experimental conditions with a perfect analytic form.

We found, in a model independent way, a space-like zero at $q^2=-11\pm2\,\mathrm{GeV}^2$ (Fig. 4a). The comparison between the models previously described [1, 6, 7, 9, 10] and our result, reported in Fig. 4b, shows that, in spite of the agreement in the space-like region, where all these models describe the polarization data, their continuations in the time-like region are far each other. Another interesting outcome of our computation is the space-like and time-like asymptotic behavior of $G_{\rm E}^p(q^2)/G_{\rm M}^p(q^2)$. According to the Phragmèn–Lindelöff theorem, that we have implemented by imposing a vanishing asymptotic value for the imaginary part of $R(q^2)$, we achieved a real time-like limit for the ratio as $q^2\to+\infty$. As shown in Fig. 5 (without and with comparison with the other models) the space-like and time-like asymptotic limits have in modulus the same value, but they have opposite sign, i.e.

$$\lim_{q^2\to\pm\infty}\frac{G_{\rm E}^p(q^2)}{G_{\rm M}^p(q^2)}=\pm1\,. \tag{11}$$

The scaling law, providing $G_{\rm E}^p\simeq G_{\rm M}^p$, that, in light of the new polarization data, is no more valid at low $|q^2|$, has been in some way restored, even if in modulus and in a "double" asymptotic regime. In addition, the Phragmèn–Lindelöff theorem predicts for the phase

$$\Phi(\infty)=(Z-P)\pi\,, \tag{12}$$

where Z and P are the number of zeros and poles of $R(q^2)$. Since we have $R(-\infty)=|R(\infty)|\mathrm{e}^{\mathrm{i}\Phi(\infty)}=-|R(\infty)|$, and being $P=0$, we obtain a further confirmation of the presence

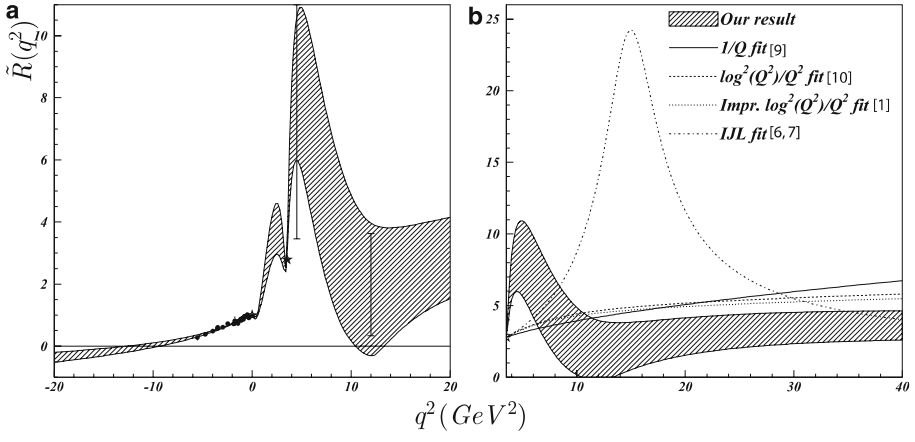

Fig. 4. a Result of the dispersive technique for the ratio $R(q^2)$ in the full data region. The lined band represents the error. **b** Ratio $R(q^2)$ in the time-like region with $q^2\geq s_p$ and comparison among various models ($Q^2\equiv-q^2$). As in Fig. 1 the *full circles* are the data from Jlab and MIT-Bates, while the two time-like intervals are from FENICE, DM2 and E835. The *stars* represent the theoretical constraints. The label $\tilde{R}(q^2)$ of the ordinate axis is defined as $\tilde{R}(q^2)=R(q^2)$ for $q^2\leq s_\pi$ and $\tilde{R}(q^2)=|R(q^2)|$ for $q^2>s_\pi$

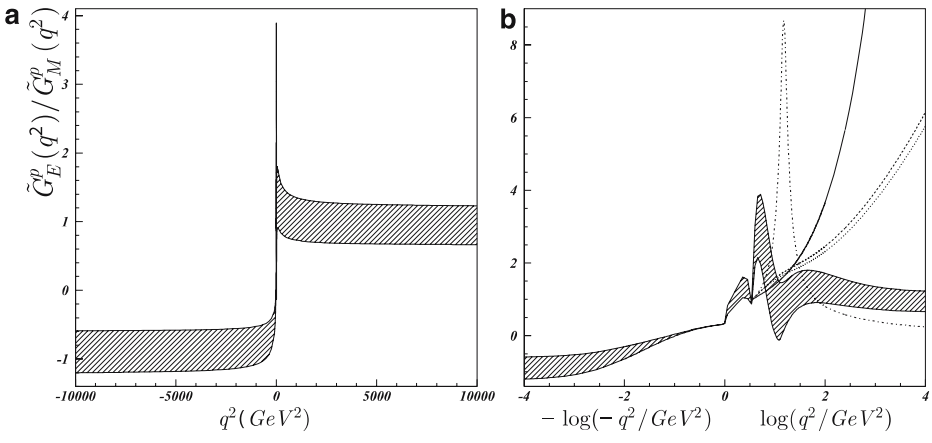

Fig. 5. a Ratio $G_{\rm E}^p(q^2)/G_{\rm M}^p(q^2)$ over a wide range of q^2. The lined band represents the error. **b** The result is compared with other models (same references as Fig. 4) in logarithmic scale for q^2. The label $\tilde{G}_{\rm E}^p(q^2)/\tilde{G}_{\rm M}^p(q^2)$ of the ordinate axis is defined as $\tilde{G}_{\rm E}^p(q^2)/\tilde{G}_{\rm M}^p(q^2) = G_{\rm E}^p(q^2)/G_{\rm M}^p(q^2)$ for $q^2 \leq s_\pi$ and $\tilde{G}_{\rm E}^p(q^2)/\tilde{G}_{\rm M}^p(q^2) = |G_{\rm E}^p(q^2)/G_{\rm M}^p(q^2)|$ for $q^2 > s_\pi$

of a zero of $R(q^2)$ (or at least an odd number of zeros). As a direct consequence of the limit of (11), we give also a prediction (Fig. 6) for the ratio between Pauli and Dirac ff's:

$$\lim_{q^2\to\infty} \tau \frac{F_2^p(q^2)}{F_1^p(q^2)} = -0.2 \pm 0.3\,, \tag{13}$$

therefore $F_2^p(q^2)/F_1^p(q^2)$ scales at least like $(1/q^2)$ as q^2 diverges.

The complete knowledge of the function $R(q^2)$ allows us to give predictions concerning quantities depending explicitly on real and imaginary part (or on modulus and phase) of ff's. In particular, we can foresee quantities like the ratio between Pauli and Dirac ff's and the polarization observables. In the space-like region, the scattering of polarized leptons on a proton target gives non-trivial polarization effects even if the target is unpolarized. The polarization of the outgoing proton, in this case, depends on the product of electric and magnetic ff's, which in this region are real.

In the time-like region, i.e. when we consider the annihilation $e^+e^- \to p\overline{p}$, the complex structure of the ff's give rise to special polarization effects: the outgoing proton may experience a polarization even if there are no polarized leptons in the initial state. This polarization will be determined by the relative phase of $G_{\rm E}^p(q^2)$ and $G_{\rm M}^p(q^2)$, that, in our case, is just the phase $\Phi(q^2)$ of $R(q^2)$.

The time-like polarization vector $\mathcal{P}$ has the components [11]

$$\begin{aligned}
\mathcal{P}_y(q^2) &= -\frac{\sin(2\theta)|R(q^2)|\sin(\Phi(q^2))}{D\sqrt{\tau}}, \\
\mathcal{P}_x(q^2) &= -P_e\frac{2\sin(\theta)|R(q^2)|\cos(\Phi(q^2))}{D\sqrt{\tau}}, \\
\mathcal{P}_z(q^2) &= P_e\frac{2\cos(\theta)}{D},
\end{aligned} \tag{14}$$

with

$$D = \frac{1+\cos^2(\theta)+\frac{1}{\tau}|\tau|^2\sin^2(\theta)}{\mu_p}\,, \tag{15}$$

where z is the direction of the outgoing proton in the center of mass system and y is orthogonal to the scattering plane, P_e is the longitudinal polarization of the initial lepton and θ is the scattering angle. As already said, the y-polarization $\mathcal{P}_y$ does not depend on P_e, while the longitudinal polarization does not depend on the phase Φ. In the pictures of Fig. 7 our predictions and those of the other considered models [1, 6, 7, 9, 10], for the components of the polarization vector are shown. Once again, models which agree in the space-like region give different predictions in the time-like region.

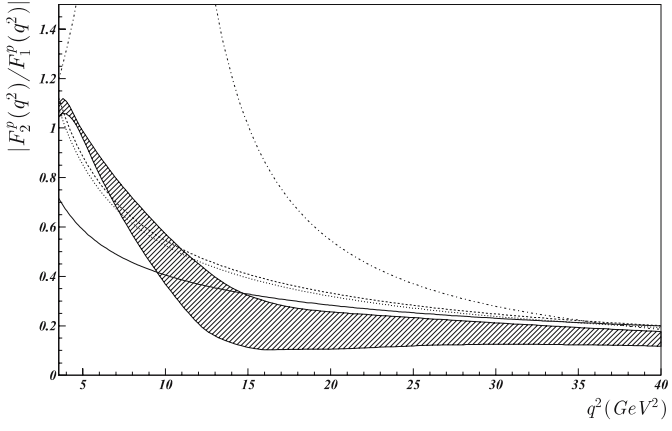

Fig. 6. Ratio $|F_2^p(q^2)/F_1^p(q^2)|$, prediction of the dispersive approach (*lined band*) compared with the other models (same references as Fig. 4)

4 Conclusions and perspectives

We have used a dispersive approach to construct an expression for the ratio $R(q^2)$, defined in the whole q^2 complex plane, which verifies all the constraints imposed by the theory (analyticity, asymptotic behavior, etc.) and by the data available at this moment. The full knowledge of the function $R(q^2)$ allows one to formulate a wide range of predictions. In particular, in the time-like region, dominance of the electric form factor near threshold, fading away soon, as well as an oscillating pattern is predicted (see Fig. 4),

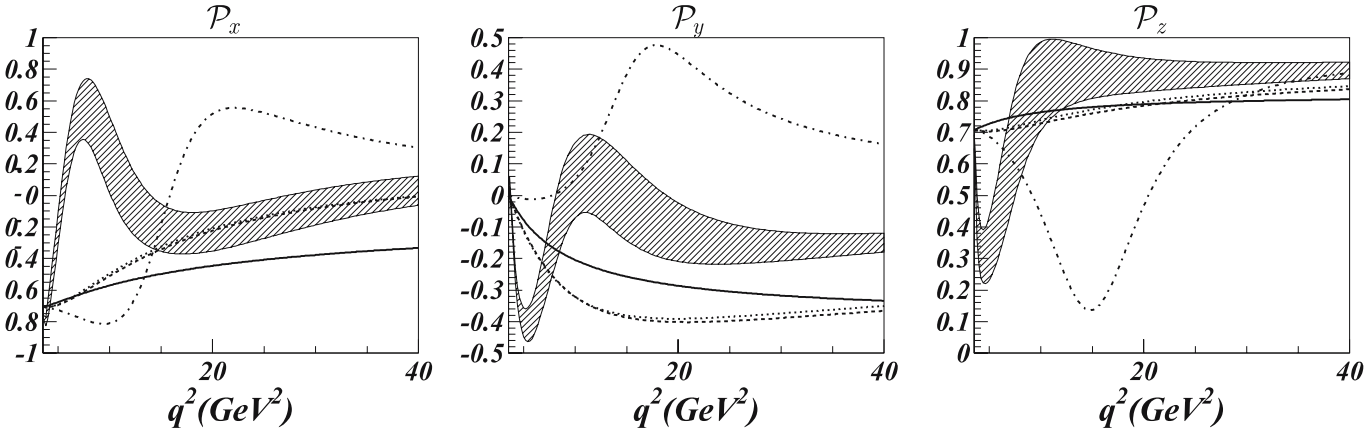

Fig. 7. Predictions for polarizations $\mathcal{P}_x$, $\mathcal{P}_y$ and $\mathcal{P}_z$ in the time-like region (*lined bands*) compared with those of the other models (same references as Fig. 4). The plots are for the scattering angle $\theta = 45^\circ$ and electron polarization $P_e = 1$

that could be interpreted as a resonance residual, surviving up to the smoothing expected in the ratio. Also the ratio between Dirac and Pauli ff's is predicted as well as a definite nucleon polarization. The other prediction that should be confirmed or refuted soon is the presence of the space-like zero, that we estimate at $q^2 = -11 \pm 2\,\mathrm{GeV}^2$, in agreement with [39]. New polarization measurements are scheduled at Jlab to push down the space-like limit at $q^2 \simeq -10\,\mathrm{GeV}^2$ [40].

Anyway, the measurement of $|R(q^2)|$ and of the polarizations [see (14)] in the time-like region would have a crucial significance not only to disentangle the models, but also to gain a rather complete experimental knowledge of the proton ff's.

Acknowledgements. We warmly acknowledge S. Brodsky, S. Dubnicka, F. Iachello, G. Pancheri, Y. Srivastava for many important suggestions and discussions. We also acknowledge the DM2, E835 and FENICE collaborations for allowing partial use of their data. After this paper had been sent for publication new data have been presented by the BaBar collaboration [41], that corroborate our conclusions.

References

1. S.J. Brodsky et al., Phys. Rev. D **69**, 054 022 (2004)
2. J. Arrington, Phys. Rev. C **69**, 022 201 (2004); F. Iachello, Eur. Phys. J. A **19**, 129 (2004); F. Iachello, Q. Wan, Phys. Rev. C **69**, 055 204 (2004); R. Bijker, F. Iachello, Phys. Rev. C **69**, 068 201 (2004)
3. M.K. Jones et al., Phys. Rev. Lett. **84**, 1398 (2000); O. Gayou et al., Phys. Rev. C **64**, 038 202 (2001); O. Gayou et al., Phys. Rev. Lett. **88**, 092 301 (2002)
4. R.C. Walker et al., Phys. Rev. D **49**, 5671 (1994); L. Andivahis et al., Phys. Rev. D **50**, 5491 (1994); J. Litt et al., Phys. Lett. B **31**, 40 (1970); C. Berger et al., Phys. Lett. B **35**, 87 (1971); L.E. Price et al., Phys. Rev. D **4**, 45 (1971); W. Bartel et al., Nucl. Phys. B **58**, 429 (1973)
5. M.N. Rosenbluth, Phys. Rev. **79**, 615 (1950)
6. F. Iachello, A.D. Jackson, A. Lande, Phys. Lett. B **43**, 191 (1973)
7. M. Gari, W. Krumpelmann, Z. Phys. A **322**, 689 (1985); E.L. Lomon, Phys. Rev. C **66**, 045 501 (2002); C **64**, 035 204 (2001)
8. T.H.R. Skyrme, Proc. Roy. Soc. A **260**, 127 (1961)
9. J.P. Ralston, P. Jain, Phys. Rev. D **69**, 053 008 (2004); J.P. Ralston, P. Jain, R.V. Buniy, AIP Conf. Proc. **549**, 302 (2000); G.A. Miller, M.R. Frank, Phys. Rev. C **65**, 065 205 (2002); M.R. Frank, B.K. Jennings, G.A. Miller, Phys. Rev. C **54**, 920 (1996); G. Holzwarth, Z. Phys. A **356**, 339 (1996); F. Cardarelli, S. Simula, Phys. Rev. C **62**, 065 201 (2000); S. Boffi et al., Eur. Phys. J. A **14**, 17 (2002)
10. A.V. Belitsky, X. Ji, F. Yuan, Phys. Rev. Lett. **91**, 092 003 (2003)
11. A.Z. Dubnickova, S. Dubnicka, M.P. Rekalo, Nuovo Cim. A **109**, 241 (1996)
12. M. Gourdin, Phys. Rep. **11**, 29 (1974)
13. R. Baldini et al., Eur. Phys. J. C **11**, 709 (1999)
14. G.F. Chew et al., Phys. Rev. **110**, 265 (1958); P. Federbush, M.L. Goldberger, S.B. Treiman, Phys. Rev. **112**, 642 (1958); S.D. Drell, F. Zachariasen, *Electromagnetic structure of nucleons* (Oxford, University Press 1960); J.S. Ball, D.Y. Wong, Phys. Rev. **130**, 2112 (1963); M.W. Kirson, Phys. Rev. **132**, 1249 (1963); J.S. Levinger, C.P. Wang, Phys. Rev. B **136**, 733 (1964); J.S. Levinger, R.F. Peierls, Phys. Rev. B **134**, 1341 (1964); J.S. Levinger, C.P. Wang, Phys. Rev. B **138**, 1207 (1965); B.A. Orman, Phys. Rev. B **138**, 1308 (1965); B.A. Orman, Phys. Rev. **145**, 1140 (1966); G.L. Kane, R.A. Zdanis, Phys. Rev. **151**, 1239 (1966); F. Chilton, F.J. Uhrhane, Bull. Am. Soc. **11**, 396 (1966); J.E. Bowcock, W.N. Cottingham, J.G. Williams, Nucl. Phys. B **3**, 95 (1967); G. Höhler et al., Nucl. Phys. B **114**, 505 (1976); H.W. Hammer, Ulf-G. Meißner, D. Drechsel, Phys. Lett. B **385**, 343 (1996); P. Mergell, Ulf-G. Meißner, D. Drechsel, Nucl. Phys. A **596**, 367 (1996); H.W. Hammer, Ulf-G. Meißner, Eur. Phys. J. A **20**, 469 (2004)
15. N. Cabibbo, R. Gatto, Phys. Rev. **124**, 1577 (1961); V. Wataghin, Nucl. Phys. B **10**, 107 (1969); J.G. Körner, M. Kuroda, Phys. Rev. D **16**, 2165 (1977); P. Cesselli, M. Nigro, C. Voci, Proc. of Workshop on Lear Physics Erice (1982); M. Van Der Velde, M.I. Polikarpov, J. Nucl. Phys. **35**, 180 (1982); E. Etim, A. Malecki, Nuovo Cim. A **104**, 531 (1991); M.M. Giannini, E. Santopinto, M.I. Kri-

voruchenko, Proc. Int. Conf. on "Meson and Nuclei at Intermediate Energies" (Dubna, 1994)
16. E.C. Titchmarsh, *The theory of functions* (University Press, Oxford 1939)
17. V.A. Matveev, R.M. Muradyan, A.N. Tavkhelidze, Lett. Nuovo Cim. **7**, 719 (1973); S.J. Brodsky, G.R. Farrar, Phys. Rev. Lett. **31**, 1153 (1973); S.J. Brodsky, G.R. Farrar, Phys. Rev. D **11**, 1309 (1975); S.J. Brodsky, P.G. Lepage, Phys. Rev. D **22**, 2157 (1980); T. Gousset, B. Pire, Phys. Rev. D **51**, 15 (1995)
18. A.A. Logunov, N. Van Hieu, I.T. Todorov, Ann. Phys. (New York) **31**, 203 (1965)
19. A. Antonelli et al., Phys. Lett. B **365**, 427 (1996); A. Antonelli et al., Phys. Lett. B **334**, 431 (1994)
20. A. Antonelli et al., Nucl. Phys. B **517**, 3 (1998)
21. B. Delcourt et al., Phys. Lett. B **86**, 395 (1979)
22. D. Bisello et al., Nucl. Phys. B **224**, 379 (1983); D. Bisello et al., Z. Phys. C **48**, 23 (1990)
23. M. Castellano et al., Nuovo Cim. A **14**, 1 (1973)
24. G. Bassompierre et al., Phys. Lett. B **68**, 477 (1977)
25. G. Bardin et al., Nucl. Phys. B **411**, 3 (1994)
26. T.A. Armstrong et al., Phys. Rev. Lett. **70**, 1212 (1993)
27. M. Ambrogiani et al., Phys. Rev. D **60**, 032 002 (1999)
28. M. Andreotti et al., Phys. Lett. B **559**, 20 (2003)
29. B.D. Milbrath et al., Phys. Rev. Lett. **80**, 452 (1998); Phys. Rev. Lett. **82**, 2221(E) (1999)
30. G. Stancari, PhD Thesis, Ferrara University (1998); M. Andreotti, Laureate Thesis, Ferrara University (2001)
31. R. Baldini et al., talk at "Baryons 2004" Paris 25–29 October, Nucl. Phys. A **755**, 286 (2005)
32. V. Blobel, Lectures given at the 1984 CERN SCHOOL OF COMPUTING, Aiguablava, Spain, September 9–22, 1984. Published in CERN Comp. School 1984:0088
33. J. Arrington, Phys. Rev. C **68**, 034 325 (2003)
34. I.A. Qattan et al., Phys. Rev. Lett. **94**, 142 301 (2005)
35. P.A.M. Guichon, M. Vanderhaeghen, Phys. Rev. Lett. **91**, 142303 (2003); P.G. Blunden, W. Melnitchouk, J.A. Tjon, Phys. Rev. Lett. **91**, 142 304 (2003); J. Arrington, Phys. Rev. C **69**, 032 201 (2004); M.P. Rekalo, E. Tomasi-Gustafsson, Eur. Phys. J. A **22**, 331 (2004); Nucl. Phys. A **740**, 271 (2004); Nucl. Phys. A **742**, 322 (2004)
36. A.V. Afanasev et al., Phys. Rev. D **72**, 013 008 (2005)
37. C.C. Kuo et al., Phys. Lett. B **621**, 41 (2005); M. Artuso et al., Phys. Rev. D **50**, 5484 (1994); H. Hamasaki et al., Phys. Lett. B **407**, 185 (1997); G. Abbiendi et al., Eur. Phys. J. C **28**, 45 (2003); P. Achard et al., Phys. Lett. B **571**, 11 (2003)
38. Frascati-LNF internal note in preparation
39. S. Dubnicka, A.Z. Dubnickova, Fizika B **13**, 287 (2004)
40. C.F. Perdrisat et al., Jefferson Lab. experiment E01-109
41. BaBar collaboration, B. Aubert et al., hep-ex/0512023